# Mass Transfer from Large Single Bubbles at High Reynolds Numbers

**TAKAYUKI NATE and D. M. HIMMELBLAU**

**University of Texas, Austin, Texas**

**Single bubbles of carbon dioxide were formed in a fixed position surrounded by a thin conical film of water flowing at average film Reynolds numbers in the range of 40 to 300. Measurements of interphase mass transfer at 32°C. and various bubble pressures agreed with predicted values only for the smallest bubbles. For larger bubbles, mixing perpendicular to the bubble interface was enhanced by waves, believed to be generated by the unstable interface. A comparison of interphase transfer coefficients between this investigation and previous work indicated that the bubbles at the lowest flow rates qualitatively fell in line with other measurements, but that the highest water flow rates gave distinctly higher coefficients.**

Measurement and prediction of interphase mass transfer from single gas bubbles have been the subject of extensive investigation. Lochiel and Calderbank (*10*) have listed most of the significant articles, as of 1964, which describe mass transfer from bubbles. Most of the previous work has been devoted to rising bubbles, either small and regularly shaped, or larger but irregularly shaped. This study was carried out at high flow rates on regularly shaped bubbles of large size (10 to 30 sq.cm. in surface area).

The bubbles used in this investigation were quite different from those studied by previous investigators in that:

1. The bubble stayed at the same position in the liquid flow field.
2. The bubble was not spherical nor oblate spheroidal, but in the shape of a cone with a hemispherical tip. The bubbles were artificial in that, although they were inherently unstable, they could be controlled in size, position, and shape by a suitable combination of liquid flow rate and flow path. The bubble was kept in a fixed position by balancing the buoyant force of the bubble with the drag force exerted by the liquid flowing in a specially designed conical cell, and a bubble supporting plate at the bottom. Because of this unique feature, it is best to describe the apparatus before presenting the mathematical model of the process.

## MASS TRANSFER APPARATUS

The apparatus shown in Figure 1 was designed to set up steady state rates of mass transfer from a gas bubble to a flowing liquid. The upper cone, being a converging flow section, provided an essentially flat velocity profile at the midpoint between the two cones. After trial and error, an inverted conical lower flow chamber was found to be a suitable type of cell to retain bubbles in a stable position within certain flow rates. Gas was introduced into the bubble through a hypodermic needle (see Figure 1) inserted to a point just below the vena contracta. Liquid which flowed around the gas bubble left the lower cone at its base through two holes.

A special feature of the bubble chamber was the adjustable "bubble chair," which was designed to keep the bottom of the bubble at a fixed point, for various water flow rates; and to make it possible to neglect mass transfer from the bottom of the bubble to the liquid, where some complicated eddy transfer might take place.

A water-repellent silicone fluid was painted on the horizontal surface of bubble chair, so that the bubble stuck firmly to it. All the lines leading to the bubble chamber were insulated and the reservoirs thermostated at 32°C.

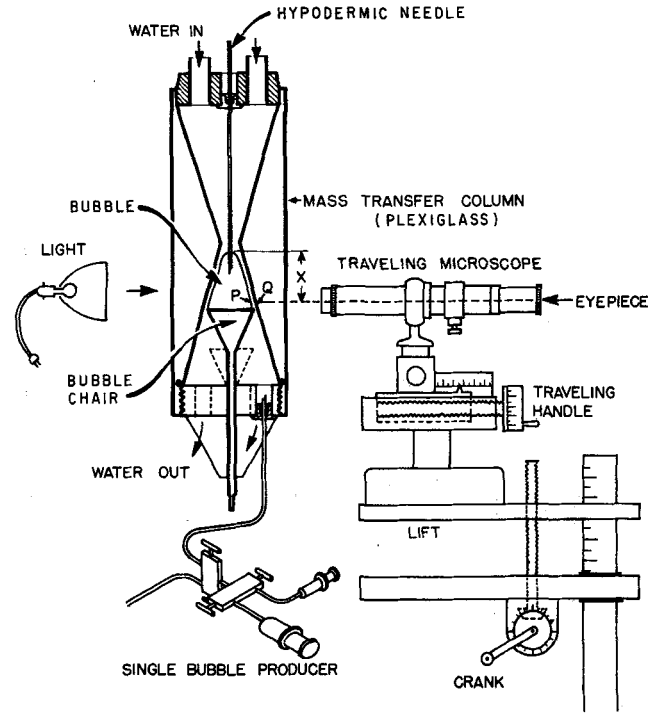


**Fig. 1. Experimental apparatus.**

Before introducing gas to the bubble through the hypodermic needle it was necessary to produce a single bubble below the vena contracta of the column for any given liquid flow rate. The bubble producing apparatus consisted of two three-way, two-stem valves and two hypodermic syringes, one for volume measurement and one for bubble injection.

Prior to the mass transfer studies, it was necessary to collect certain fundamental data concerning the gas bubble and the water film around it. The bubble surface area had to be known, the water film thickness was required for the mathematical model, refraction corrections were needed, and so forth. Also the precise calibration of the differential pressure gas flow meter leading to the hypodermic needle was necessary. All optical measurements were made with a combination of a Gaertner M-101 microscope and a M-301 micrometer slide. The details of these complicated but necessary calibration steps are reported in reference *11*. Pictures were taken of the bubbles as a check on their size.

It was also of special interest to know if the flow of water around the bubble was laminar or turbulent, and what the streamlines were like. To do this, a saturated solution of potassium permanganate was injected by a very fine hypodermic needle directly above the bubble top. In the water flow range of 115 to 800 cc./min. used in this work, it was observed that the stream of potassium permanganate solution moved in a laminar fashion down the bubble surface for most of the distance, and that it spread out as expected. However, the streamlines near the bottom portion of the bubble were often distorted by slight rotation and/or ripples.

After the preliminary experiments were completed, absorption data were taken with pure carbon dioxide first and later on with carbon dioxide-air mixtures. To supply pure gas to the bubble, all the tubing in the system was purged by carbon dioxide from a storage cylinder. A single bubble of carbon dioxide was introduced into the lower cone, but because a single bubble would not stay under the vena contracta for water flows of less than 250 cc./min. the water flow was set at approximately 300 cc./min. until after a bubble was injected and formed. Then it was possible to reduce the flow rate and yet retain the bubble.

As soon as the bubble was in place, the gas flow rate through the vertical hypodermic needle was slowly adjusted so that the bubble volume increased gradually until the bottom of the bubble stuck to the surface of bubble chair, at which time the gas flow rate was reduced slightly and adjusted as needed to maintain constant bubble size. When the bubble volume remained constant for more than 5 min., the gas absorption rate was said to have reached the steady state. At this time the reading of the gas flow into the bubble was recorded as well as the bubble size, bubble pressure, and water flow rate.

## MATHEMATICAL MODEL

Figure 2 gives the relevant coordinates for the system, a set of coordinates originally proposed by Boltze (*4*); details can be found in reference *12*. The coordinate $z$ is normal to the curve $OP$, while coordinate $x$ is measured from $O$ to the point $P$ along the bubble interface. The velocity $u$ is in the $x$ direction; $w$ is in the $z$ direction.

The steady state boundary-layer equations for rotational symmetry and axial symmetric flow in the given coordinate system (*12*) reduce to

Momentum:

$$u\frac{\partial u}{\partial x} + w\frac{\partial u}{\partial z} = -\frac{1}{\rho}\frac{\partial p}{\partial x} + \nu\frac{\partial^2 u}{\partial z^2} \tag{1}$$

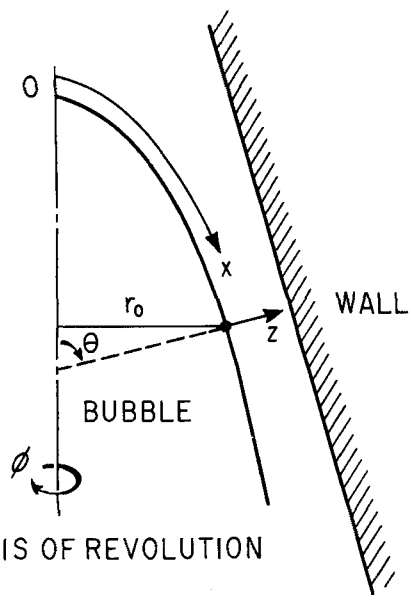


Fig. 2. Coordinate system for bubble.

$$u\frac{\partial w}{\partial x} + w\frac{\partial w}{\partial z} = \nu\frac{\partial^2 w}{\partial z^2} \tag{2}$$

Continuity:

$$\frac{\partial (r_o u)}{\partial x} + \frac{\partial (r_o w)}{\partial z} = 0 \tag{3}$$

Component mass:

$$u\frac{\partial c}{\partial x} + w\frac{\partial c}{\partial z} = D\frac{\partial^2 c}{\partial z^2} \tag{4}$$

Relations for mass transfer along a mobile axisymmetric body of revolution have been determined by Lochiel and Calderbank from Equations (3) and (4) for the following assumptions, which were met by the experimental system:

1. small boundary-layer thickness compared to radius of curvature
2. short distance of penetration of solute (compared to the water film thickness)
3. $N_{Pe} > 100$
4. $N_{Re} > 0.1$

and for the following boundary conditions on Equation (4):

$$\begin{aligned} c\ (x, 0) &= c_e \\ c\ (x, \infty) &= 0 \\ c\ (0, z) &= 0 \end{aligned}$$

For these assumptions the total transfer, taking into account the entire surface of the bubble, reduces to

$$\begin{aligned} N &= -\int_0^A D\left(\frac{\partial c}{\partial z}\right)_{z=0} dA' \\ &= 4c_e\sqrt{\pi D}\left[\int_0^{x_2} u_s r_o^2\, dx\right]^{1/2} \\ &= k_L c_e A \end{aligned} \tag{5}$$

Rather than solving the momentum balances, it was easier to use the continuity equation together with empirical measurements to obtain an approximate analytical expression for the velocity $u_s$ needed for Equation (5). From an analysis of empirical velocity distributions in the literature, the velocity was assumed to be quadratic in $z$

$$u = [a_o(x) + a_1(x)z + a_2(x)z^2] \tag{6}$$

in which the coefficients are functions of $x$ only. These coefficients were determined from three physical conditions:

1. At the mobile bubble interface, the velocity $u = u_s$ was a maximum
$$\frac{\partial u(x, 0)}{\partial z} = 0$$
2. At the chamber wall, $z = h(x)$, the velocity $u$ vanished
$$u(x, h) = 0$$
3. A mass (volumetric) balance could be written at any distance $x$ along the flow annulus for the water
$$Q = \int_0^{h(x)} u(z) 2\pi (r_o + z) dz$$

Application of these three conditions yielded the following expression for the velocity at the surface of the bubble:

$$u_s = U\frac{\left[r_o + \frac{h(x)}{2}\right]}{\left[\frac{2}{3}r_o + \frac{h(x)}{4}\right]} \tag{7}$$

$$= \frac{Q}{\pi h(x)\left[\frac{4}{3}r_o + \frac{1}{2}h(x)\right]} \qquad (7a)$$

Both $r_o$ and $h(x)$ were known functions of $x$. In the conical section of the bubble these variables were essentially linear and were formulated as

$$r_o = \alpha_1 + \alpha_2(x)$$

$$h(x) = \beta_1 + \beta_2(x)$$

The coefficients $\alpha_1$, $\alpha_2$, $\beta_1$, and $\beta_2$ were determined for each bubble from experimental measurements. The tip of the bubble could be approximated by a portion of a sphere without serious error since the interphase mass transfer across the cap of the bubble was less than 10% of the total transfer.

## RESULTS AND DISCUSSION

It was estimated that the largest error in the experimental measurements was introduced from measurements of the bubble surface area and water film thickness. These latter were found to have average deviations of about 7%, but the error in $k_L$ was less. Table 1 illustrates a series of typical replicate runs in which the average $k_L$ was 0.0237 cm./sec. and the standard deviation was 0.0012.

In the presentation and correlation of data it was desirable to calculate a Reynolds number. Since the flow rate was not uniform around the bubble, an average Reynolds number was defined as

$$(N_{Re})_{av} = \left(\frac{\rho u \delta}{\mu}\right)_{av}$$

where $\delta$ is the water film thickness between the bubble and the wall in the $z$ direction (perpendicular to the surface of the bubble). From measurements of the film thickness and bubble size, the film thickness $\delta$ was known as a function of $x$, and from Equation (6), the velocity was known as a function of $x$, as well. Consequently

$$(N_{Re})_{av} = \frac{\rho}{\mu}\frac{\int_0^{x_2} u(x)\delta(x)dx}{\int_0^{x_2} dx}$$

Figure 3 compares the predicted and measured values of the interphase mass transfer expressed in terms of the Sherwood number

$$N_{Sh} = \frac{k_L d_e}{D} = \frac{N d_e}{A c_e D}$$

vs. the average Reynolds number. The characteristic length in the Sherwood number was chosen to be the equivalent diameter of the bubble, computed from $d_e^2 = A/\pi$, but

TABLE 1. REPRODUCIBILITY OF DATA

Bubble size = 24.6 sq. cm.; water flow rate = 300 cc./min. bubble pressure measured by manometer = 760 mm. Hg

| Run No. | Carbon dioxide temperature, °C. | Atmospheric pressure, mm. Hg | $k_L$, cm./sec. |
|---|---|---|---|
| 1 | 32.0 | 745.1 | 0.0234 |
| 2 | 31.6 | 741.8 | 0.0230 |
| 3 | 32.0 | 749.0 | 0.0237 |
| 4 | 32.2 | 744.7 | 0.0245 |
| 5 | 31.9 | 747.0 | 0.0240 |
| 6 | 32.5 | 750.1 | 0.0237 |

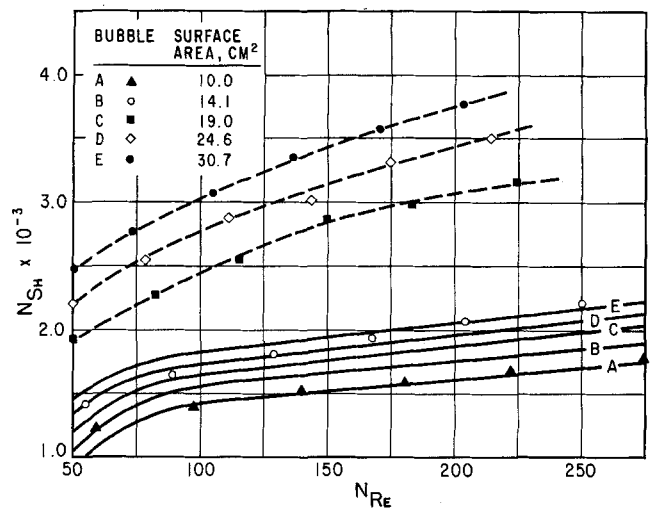


Fig. 3. Predicted and measured interphase transfer for 760 mm. Hg bubble and 32°C.

just as well could have been the height of the bubble or one of the other methods for picking a characteristic length for nonspherical bubbles mentioned below.

Only for the smallest size bubble were the experimental and predicted Sherwood numbers in agreement. All larger size bubbles had enhanced interphase mass transfer over the predicted transfer. Investigation into the discrepancy revealed a very interesting feature of the bubble which has been recorded and remarked on before, namely, the ringlike waves which existed on the rear one-third to one-half of the larger bubbles (see Figure 4). The same type of standing waves has been photographed on long bubbles rising in vertical tubes by van Heuven and Beek (*14*) and has been described by Barr (*2*) in some detail. Van Heuven and Beek ascribed the waves to a gradient of surface tension on the lower part of the bubble. While surface-active agents can be swept back to the rear of a bubble, in this work it appeared as if surface-active agents should be swept off the rear of the bubble into the stream.

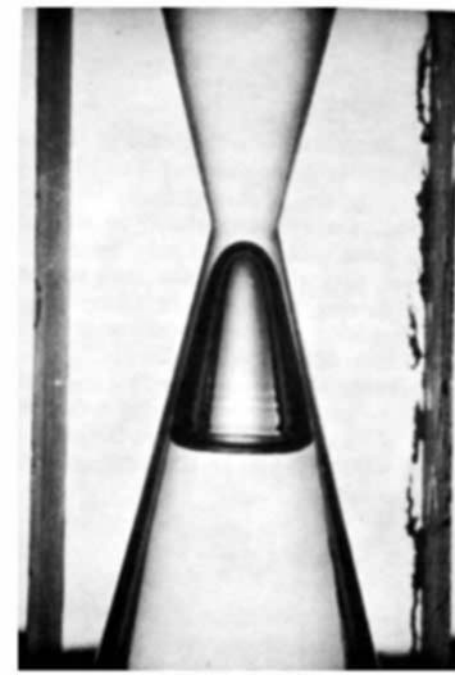

Fig. 4. Flow of water at 400 cc./min. past bubble 19.3 sq.cm. in area. Note standing waves on lower portion of bubble.

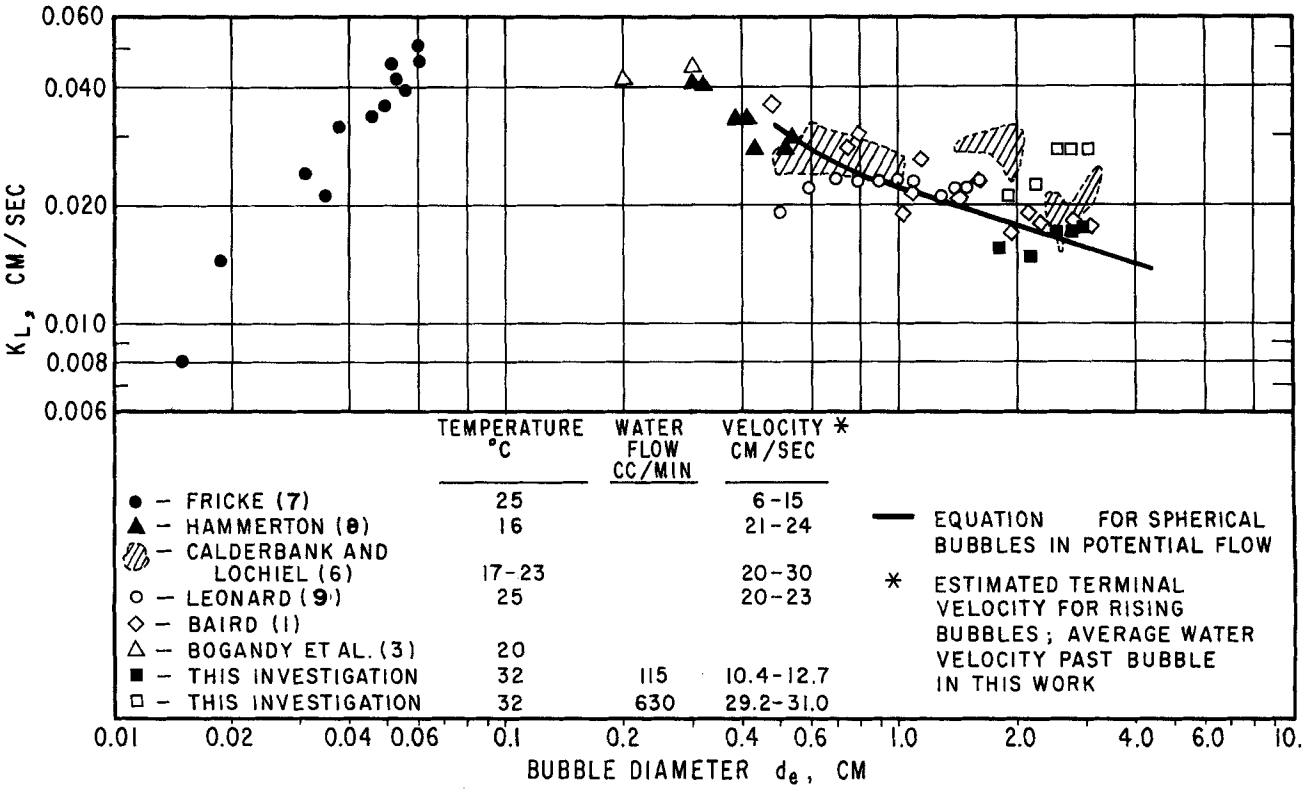


**Fig. 5. Mass transfer coefficient comparison for carbon dioxide-water system.**

Instead it is believed these waves or ripples were engendered by instability at the free interface. In principle, but probably not in practice, the stability problem for a thin inclined film of liquid bounded underneath by a less dense phase and above by a wall could be solved asymptotically for large values of the Reynolds number. Such a film would be inherently unstable for finite wave numbers of disturbances. Some rough calculations made with the approximate method of Schechter and Himmelblau (*13*) have indicated stability exists at a Weber number of less than about 4. The value of the Weber number

$$N_{We} = \frac{\rho U^2 L}{\sigma}$$

depends to some extent on the definition of the velocity $u$ and length $L$, but was in the range of 2 to 10 for the bubbles in this investigation if $L$ represented the height of the bubble and $u$ the average velocity in the thin water film. Although these numbers can only be given qualitative significance, they do point out that the stationary bubble in the flowing fluid had an inherently unstable interface which added convective mixing in the $z$ direction to the diffusion of the carbon dioxide.

Figure 5 is the usual method of portraying values of $k_L$ for bubbles. To be consistent with earlier work, the equivalent diameter $d_e$ is defined for Figure 5 as the diameter of a sphere of volume equal to the volume of a bubble at atmospheric pressure:

$$d_e = \left(\frac{6V_B}{\pi}\right)^{1/3}$$

Because experimental conditions of the bubble in this investigation were different from those used by previous investigators, the mass transfer coefficients can be compared only roughly. However, by selecting bubbles from previous investigations which had terminal velocities of the same value as the average water velocity in this work, it was possible to compare these data as illustrated in Figure 5. Rising bubbles with values of $d_e$ greater than 1 cm. form distorted fluctuating shapes as they rise, and are only roughly correlated by the equation of Boussinesq (*5*), $N_{Sh} = 1.13\, N_{Pe}^{1/2}$, but small mobile bubbles should follow the curve indicated by the solid line in the figure fairly well.

It will be observed that at the lowest flow rate (115 cc./min.), for which the predicted and experimental Sherwood numbers agreed in Figure 3, the points fall reasonably near the theoretical curve for spheres. At the highest flow rate, the mass transfer coefficients are distinctly higher than those for equivalent spherical bubbles.

Other investigators' points represent data for bubbles rising in a stationary liquid at their terminal velocities. These velocities are equivalent to the lowest flow rate in this investigation, 115 cc./min., the flow rate at which the drag on the bubble just balanced the buoyancy effects. Higher flow rates in this work had no realizable equivalent for free bubbles, because at these flow rates the bubble was driven down on the bubble chair and would have descended if it were not for the support provided by the bubble chair.

The effect of the total pressure in the bubble must be distinguished from the effect of the carbon dioxide partial pressure in the bubble. Changing the total pressure in the bubble changed only its shape, with the result that the water film thickness between the bubble and flow chamber wall changed. It was found that the higher the total bubble pressure, the higher was the average linear velocity of water flowing around the bubble when the bubble surface area and water flow rate were fixed.

The effect of the partial pressure of carbon dioxide in mixed carbon dioxide-air bubbles vs. the mass transfer coefficient $k_L$ is shown in Figure 6. The partial pressure of the carbon dioxide was calculated from mass spectrograph analyses of the carbon dioxide-air mixtures in the bubbles. Figure 6 indicates that $k_L$ was almost indepen-

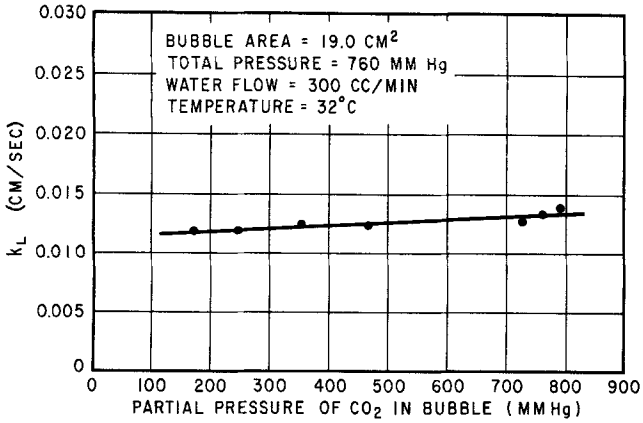


**Fig. 6. $k_L$ vs. partial pressure of carbon dioxide.**

dent of the partial pressure of carbon dioxide, perhaps slightly decreasing with decreasing carbon dioxide partial pressure. If the gas in the bubble is in equilibrium with that in the liquid interface at all times, Figure 6 demonstrates that the right-hand side of Equation (5), based on the driving force concept of interphase mass transfer, could be applied successfully. The liquid phase resistance essentially controlled the transfer, as expected.

If the Sherwood number is redefined in terms of an average water film thickness $\delta_{av}$, $N_{Sh} = (k_L\delta_{av}/D)$, then the bubble data can be roughly correlated as in Figure 7. For a fixed bubble size the data are fairly linear, but all sizes of bubbles do not fall on the same line. Therefore it was not feasible to set up one equation to correlate adequately all the mass transfer data for all sizes of bubbles and all pressures.


## ACKNOWLEDGMENT

This work was supported in part by the University Research Institute.


## NOTATION

$a_0$, $a_1$, $a_2$ = coefficients in velocity distribution, Equation (6)
$A$ = bubble surface area
$c$ = molar concentration of solute (gas) in solvent (water)
$c_e$ = saturated molar concentration of gas in solvent
$d_e$ = equivalent diameter
$D$ = diffusion coefficient of solute in solvent
$h$ = film thickness measured from $z = 0$
$k_L$ = interphase mass transfer coefficient based on liquid phase driving force
$L$ = characteristic length
$N$ = interphase molar transfer rate of solute
$N_{Pe}$ = Peclet number $(LU/D)$
$N_{Re}$ = Reynolds number $(LU\rho/\mu)$
$N_{Sh}$ = Sherwood number, $(k_Ld_e/D)$ or $(k_L\delta_{av}/D)$
$N_{We}$ = Weber number $(\rho u^2L/\sigma)$
$p$ = pressure
$Q$ = volumetric water flow rate
$r_o$ = polar radius, defined in Figure 2
$u$ = tangential velocity component (in $x$ direction)
$u_s$ = tangential velocity at surface of bubble $(z = 0)$
$U$ = characteristic velocity (average velocity)
$V_B$ = volume of bubble
$w$ = velocity component in $z$ direction
$x$ = distance along interface from front stagnation point

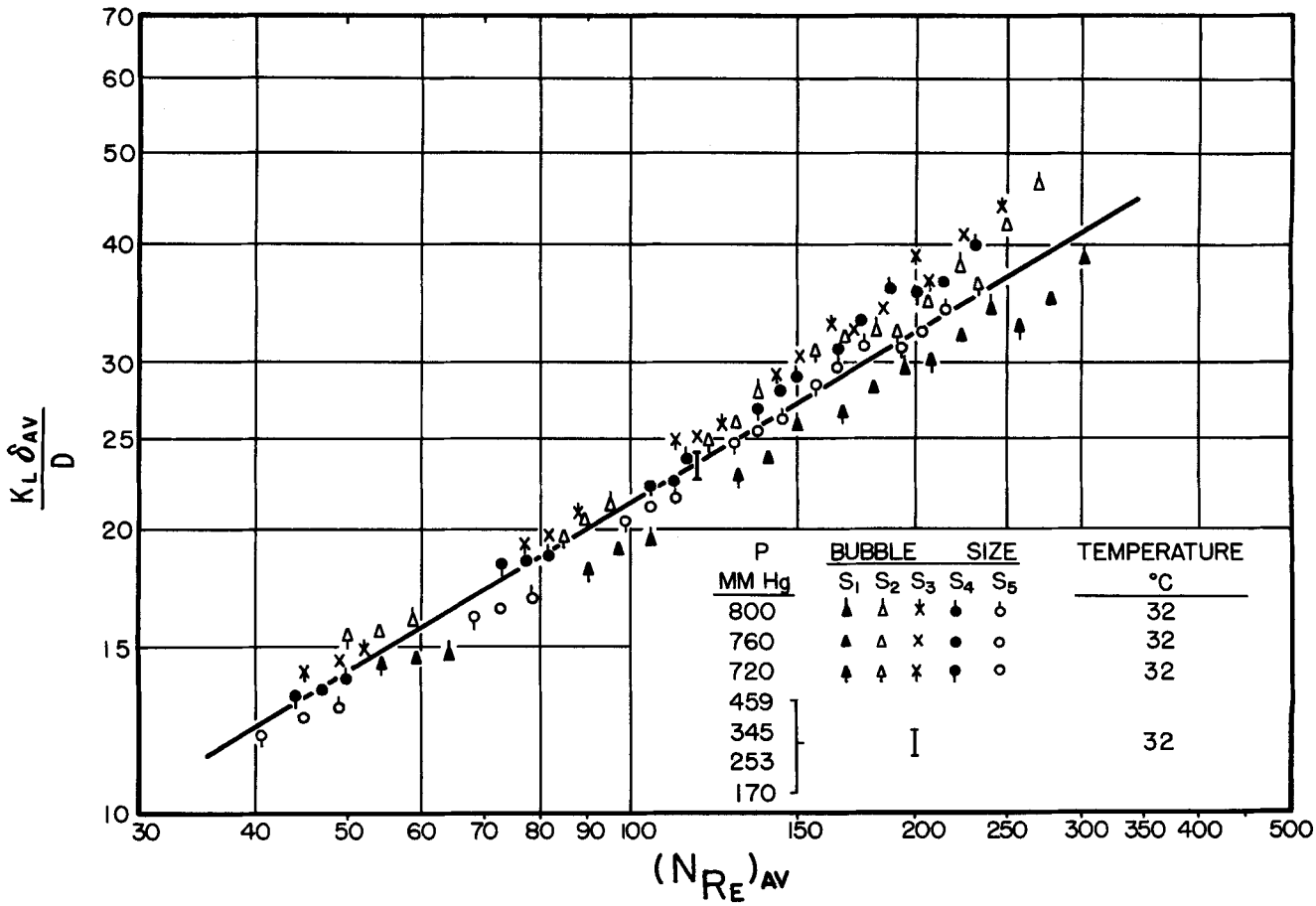


**Fig. 7. Correlation of $k_L$ data.**

$x_2$ = length of bubble interface from $x = 0$
$z$ = direction perpendicular to bubble surface measured from bubble surface

**Greek Letters**

$\alpha, \beta$ = constants
$\delta$ = water film thickness
$\mu$ = coefficient of shear viscosity
$\nu$ = kinematic viscosity ($\mu/\rho$)
$\rho$ = fluid density
$\sigma$ = coefficient of interfacial tension

**Subscript**

av = average

## LITERATURE CITED


1. Baird, M. H. I., Ph.D. thesis, Cambridge Univ. (1960).
2. Barr, G., *Phil. Mag.*, 1. 395 (1926).
3. Bogandy, L., W. von Rutsch, and I. N. Stranski, *Chem. Ing. Tech.*, **31**, 580 (1959).
4. Boltze, E., Grenzschichten an Rotationskörpern, Göttingen (1908).
5. Boussinesq, J., *J. Math*, **6**, 285 (1905).
6. Calderbank, P. H., and A. C. Lochiel, *Chem. Eng. Sci.*, **19**, 485 (1964).
7. Fricke, R., *Z. Phys. Chem.*, **104**, 363 (1923).
8. Hammerton, D., and F. H. Garner, *Trans. Inst. Chem. Engrs.*, **32**, 518 (1954).
9. Leonard, J. H., Ph.D. thesis, Univ. Pittsburgh, Pa. (1961).
10. Lochiel, A. C., and P. H. Calderbank, *Chem. Eng. Sci.*, **19**, 471 (1964).
11. Nate, T., M.S. thesis, Univ. Texas, Austin (1962).
12. Rosenhead, L., "Laminar Boundary Layers," Chap. 8, Oxford Univ. Press (1963).
13. Schechter, R. S., and D. M. Himmelblau, *Phys. Fluids*, **8**, 1431 (1965).
14. Van Heuven, J. W., and W. J. Beek, *Chem. Eng. Sci.*, **18**, 377 (1963).



*Manuscript received August 17, 1966; revision received November 22, 1966; paper accepted November 22, 1966. Paper presented at AIChE Salt Lake City meeting.*


# Diffusion Coefficients of Hydrogen and Helium in Water


**R. T. FERRELL and D. M. HIMMELBLAU**

**University of Texas, Austin, Texas**



**Measurements of laminar dispersion in a capillary have been used to determine the molecular diffusion coefficients of hydrogen and helium dissolved in water over the temperature range of 10° to 55°C. Literature correlations did not predict realistic values of the diffusivities for the hydrogen—water and helium—water binaries. A statistical analysis of the experimental diffusion coefficients indicated that they could be related to the absolute temperature by a semiempirical correlation, which may be considered an extension of the well-known Wilke-Chang correlation. This relation was based on the absolute reaction rate model of liquids.**


Knowledge of molecular diffusion coefficients of sparingly soluble gases dissolved in liquids is important in many fields. The theorist employs these values in testing existing or proposed liquid state theories for low molecular weight solutes. The experimentalist often uses diffusion coefficients of dissolved gases as an aid in interpreting laboratory investigations. Finally, diffusion coefficients are useful to the engineer in his investigation and prediction of mass transfer.

With the exception of water as the liquid solvent, very little experimental data have been reported (*14*), and even for water, there is a wide range in the diffusivities for dissolved hydrogen and helium. In addition, in the majority of experiments the value of the diffusion coefficient has been obtained at only one temperature.

Experimental determination of diffusion in liquids is inherently difficult because the diffusion process in liquids is so slow. This problem is magnified in the case of sparingly soluble gases because of the difficulty in determining accurately trace quantities of dissolved gas (*18*). For example, the saturation concentration of helium in water at standard conditions is less than 1 p.p.m. on a mole basis.

The experimental method used in this investigation was adapted from that developed originally by Taylor (*24, 25*). The technique essentially consists of imposing a known concentration change of solute on a fluid in laminar flow passing through a long slender duct. The molecular diffusivity can be obtained from measurements of the concentration distribution downstream from the injection point. The time required to carry out an experimental run in such an apparatus, while not as short as in a liquid jet, was considerably less than for a diaphragm cell.

## MATHEMATICAL MODEL OF PHYSICAL SYSTEM

In dilute solutions of gases dissolved in liquids, the effect of gas concentration on the system density and viscosity is so small that these parameters can be assumed to be the same as those of the solvent. Consequently, in an isothermal laminar flow system, with no chemical reactions, with the diffusion path a cylindrical duct, and with a concentration distribution possessing axial symmetry, the mass balance for fully developed flow becomes

$$\frac{\partial c^+}{\partial t} + 2u\left[1 - \frac{r^2}{R^2}\right]\frac{\partial c^+}{\partial z} = D\left[\frac{1}{r}\frac{\partial}{\partial r}\left(r\frac{\partial c^+}{\partial r}\right) + \frac{\partial^2 c^+}{\partial z^2}\right] \quad (1)$$

For a step change in the input concentration imposed on the fluid, the initial and boundary conditions accompanying Equation (1) are